2008 IEEE International Conference on
Robotics and Automation
Pasadena, CA, USA, May 19-23, 2008

Controlling Shoulder Impedance in a Rehabilitation Arm Exoskeleton

Craig R. Carignan, Michael P. Naylor, and Stephen N. Roderick

Abstract— **A control methodology is developed for modulating shoulder impedance in an arm exoskeleton during physical therapy. Setting the remote center of compliance at the shoulder will allow the exoskeleton to enact resistance training protocols that strengthen the rotator cuff and other joint musculature supporting the shoulder complex. The rotational kinematics for the shoulder are first derived, and then the torques applied at the shoulder are estimated using force sensors placed at the hand and elbow interfaces. Impedance and admittance control schemes are both developed for realizing isolateral strengthening exercises, and some preliminary experimental results are presented for implementation on an arm exoskeleton currently under development.**

I. INTRODUCTION

In most manipulator applications, the remote center of compliance is located at the tool tip and controlled using force readings from a sensor located in the wrist. Likewise, exoskeletons developed for virtual reality (VR) applications usually reflect forces at the hand resulting from interaction with virtual environments [1]. This type of force reflection can be met by using a central controller to simultaneously move all of the exoskeleton joints to exert a desired force at the hand. However, this strategy is ineffective for rehabilitation applications where individual arm joints are being targeted for physical therapy.

In a rehabilitation arm exoskeleton, the remote center of compliance is any joint-muscle group in the arm being targeted for therapy. For example, during the shoulder extension exercise shown in Fig. 1, the resistance about the shoulder lateral axis needs to be controlled by the exoskeleton over the range of motion. An additional complication is that a force-torque sensor placed at the wrist or hand does not alone provide enough information to determine the torques in the shoulder joint. Therefore alternative force sensor emplacement strategies also need to be investigated.

In this article, dual impedance-admittance control approaches are investigated for modulating impedance in the shoulder joint during exercise therapy. The shoulder-axis can either be fixed or vary with configuration of the arm. Impedance control schemes are explored that use force-torque sensors placed at the hand and elbow to estimate the applied forces. Some preliminary test results are presented for implementing impedance control for realizing isolateral exercises.

This work was support by the U.S. Army Telemedicine and Advanced Technology Research Center (TATRC), Ford Detrick, Maryland

C. Carignan is a research associate professor with the Imaging Science and Information Systems Center, Georgetown University, Washington DC 20057 USA crc32@georgetown.edu

M. Naylor and S. Roderick were faculty research associates with the Space Systems Laboratory, University of Maryland, College Park MD 20740 USA; Naylor is now a robotics engineer with Accuray, Inc., Sunnyvale CA mnaylor@accuray.com and Roderick is a consulting engineer snrkiwi-2007@yahoo.com

Fig. 1. The MGA Exoskeleton has five powered joints including a three-axis intersecting shoulder and a scapula elevation joint.

II. PREVIOUS WORK

Most arm exoskeletons built to-date were developed as either force-reflecting master arms for teleoperation or as haptic devices for virtual reality (VR) applications [1]. In these applications, "contact" forces are imparted at the handle of the exoskeleton that replicate forces sensed by a slave arm or by interaction with a virtual environment. A basic form of impedance control is usually implemented in which the Cartesian forces at the handle are mapped into joint torque commands using the Jacobian [10]. This approach eliminates the need to compute the inverse kinematics and is stable at low impedances.

The main drawback of impedance control is that good force replication at the handle requires compensation of the natural dynamics of the exoskeleton, such as gravity loading and drive friction. A force loop wrapped around the force sensor can reduce unmodeled effects [2], but it can also easily destabilize the system. The *Exoskeleton Arm-Master* [1] and the *L-Exos Exoskeleton* [7] are classic examples of exoskeletons that use this approach.

An alternative approach called "admittance" control has primarily been used to control manipulators used as large-reach haptic devices [3], [5]. In this approach, the sensed force at the handle is used as the input to a desired impedance

model, which outputs a desired motion to be imparted at the hand. The Cartesian position is mapped into joint position commands using the inverse kinematics, which are then input to a proportional-derivative (PD) servocontroller to drive the joints to the desired position.

The main advantage of the admittance approach is that the high gains of the joint position servo-loop are used to reject unmodeled dynamics without resorting to model feed-forward. However, it has the major drawback of instability for high admittance (low impedance), which is the opposite of impedance control [9]. The *Sensor Arm* [11] is an example of an exoskeleton implementing this approach, and the more recent *ARMin Exoskeleton* [12] appears to be able to operate in either admittance or impedance mode.

Almost all exoskeleton designs incorporate a six-axis force sensor at the gripper for determining forces applied at the hand [7]. Some designs use force-torque sensors mounted on the links to obtain forces at other locations along the arm. The *ARMin* reacts loads to the distal end of the forearm link through force-torque sensor attached to a wrist cuff [12]. The *Sensor Arm* [11] uses concentric rings connected by strain gauges to determine forces applied by the arm, where the inner ring is secured to the limb using an inflatable bladder. Attempting to use torque cells at the exoskeleton joints to derive torques in the human joints is fraught with difficulties because the exoskeleton joints do not align with the human joints and the internal joint dynamics corrupt the readings. Thus this approach is rarely used.

III. SHOULDER KINEMATICS

The human shoulder (glenohumeral) joint is a ball-and-socket joint capable of abduction/adduction, flexion/extension, and internal/external rotation as shown in Figure 2. In addition, the glenohumeral joint translates along the surface of a sphere as the humerus (upper arm) elevates producing both shoulder elevation/depression and pronation/supination (in and out of plane). The ability to replicate this "scapulo-humeral rhythm" is key to realizing natural movement of the shoulder. The exoskeleton uses three serially-connected rotational joints with intersecting axes to replicate this motion. However, the axes of rotation do not always correspond to the anatomical abduction-flexion-rotation axes.

Figure 3 shows the kinematic configuration of the MGA Exoskeleton along with and Denavit-Hartenburg (D-H) link frame assignments [6]. The D-H parameters for the kinematics are given in Table I except for the scapula joint 0 which is mounted perpendicular to the coronal plane. The angle between the z_0 and z_1 axis is $30°$, and the angle between the z_3 and z_4 axis is $45°$. The scapula, upper arm, and forearm links all have passive sliding joints to accommodate variable subject geometry: $L_S = 14.0 - 25.6$ cm, $L_U = 27.3 - 31.3$ cm, and $L_F = 30.0 - 39.0$ cm. The displacement of the force sensors along the z-axis of their respective frames are $L_{S_h} = 5.72$ cm and $L_{S_e} = 7.62$ cm.

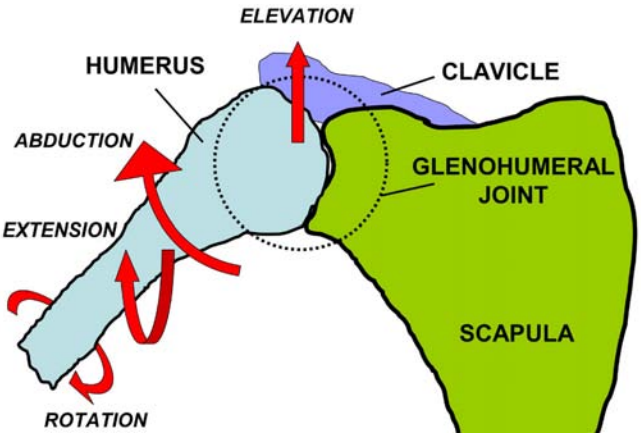

Fig. 2. Movements of the human arm and shoulder girdle.

TABLE I
D-H PARAMETERS FOR THE MGA EXOSKELETON.

link i	a_{i-1} (cm)	α_{i-1} (deg)	d_i (cm)	θ_i* home (deg)
1	0	$+30$	0	$+90$
2	0	-90	0	-105
3	0	$+90$	$\sqrt{2}L_U$	-90
4	0	-45	$-L_U$	0
5	0	-90	L_F	0

A. Arbitrary Shoulder Rotation

Shoulder rotation is defined as the orientation of the upper arm frame $\{U\}$ with respect to the body frame $\{B\}$. Frame $\{U\}$ is co-located with frame $\{4\}$ but with the z_U-axis directed along the humerus away from the shoulder. It can thus be defined as a $45°$ rotation of frame $\{3\}$ about the x_3-axis, i.e. ${}^3R_U = R_X(45°)$, followed by a translation of $-L_U/\sqrt{2}$ along the z_4-axis

$$ {}^B R_U = {}^B R_0 \, {}^0 R_3 \, {}^3 R_U \tag{1} $$

where ${}^B R_0 = R_X(-\theta_0)$. The shoulder orientation ${}^0 R_3$ relative to the base is determined by using the D-H Table to find the local link transformations ${}^i R_{i+1}$ and cascading the resulting rotation matrices for links 1-3. The direction of the humeral axis in the body frame $\{B\}$ is given by ${}^B \hat{z}_U$, the third column of ${}^B R_U$, which is used to compute the axis of rotation for internal/external shoulder rotation exercises.

B. Self-Motion Shoulder Rotation

During exercise involving translation of the hand, the free-axis of shoulder rotation is along a straight line from the shoulder to the wrist as shown in Figure 4. Because the axis passes through the wrist, rotation about this axis or "elbow orbit" produces no motion of the wrist and is thus referred to as "self-motion". The elbow "orbit" angle ϕ is defined as the angle that the plane formed by the points S, E, and W makes with the reference plane defined by the reference vector, $\hat{v}$, and the shoulder-wrist vector, p_w [8].

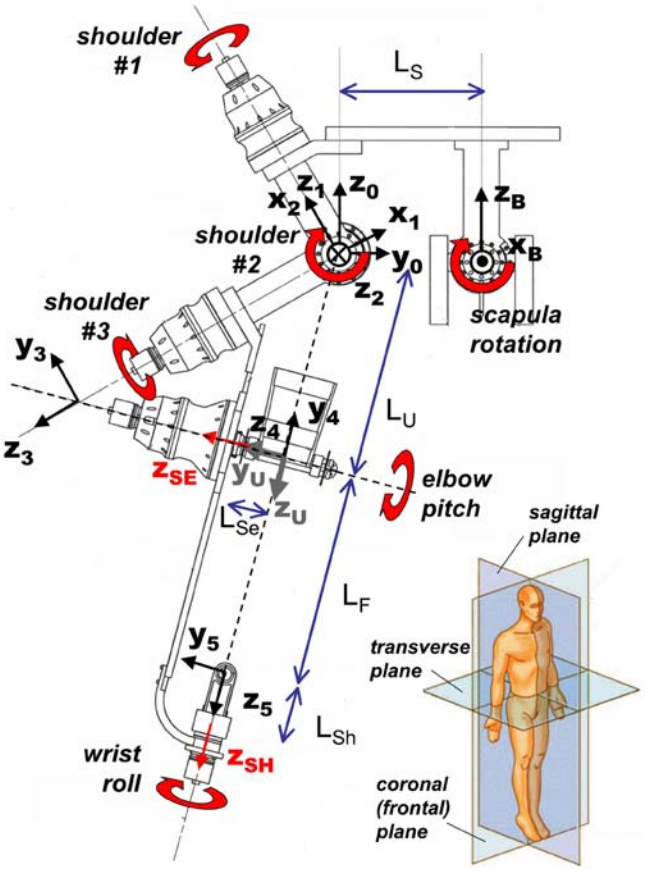

Fig. 3. MGA Exoskeleton link frame assignments shown in the frontal (coronal) plane. The exoskeleton joint axes are along the z_i-axes with rotations indicated by an arrow. The body planes are shown in the inset (http://en.wikipedia.org/wiki/Image:BodyPlanes.jpg).

Let the vectors from the shoulder to the wrist and elbow be defined as p_w and p_e, respectively, and let $\hat{v}$ denote an arbitrary fixed unit reference vector in frame 0. The roll angle of the SEW plane or "elbow orbit angle" is defined as the angle between p_p and p_ℓ

$$tan\phi \equiv \frac{\hat{p}_w^T(p_\ell \times p_p)}{{p_\ell}^T p_p} \tag{2}$$

ϕ is calculated by using the forward kinematics to compute p_w and p_e and then performing the vector operation in (2) numerically.

IV. ISOLATERAL EXERCISE CONTROL

Iso-lateral exercises are those that occur around a single rotation axis of the shoulder and closely resemble those performed manually with dumbbells, rubber tubing, and exercise machines [13]. Examples of shoulder rotation exercises include internal/external rotation and shoulder abduction/adduction as shown in Figures 5 and 6, respectively. In isolateral exercises, the motion of the shoulder joints is determined by the motion of the upper arm. In self-motion exercises, the axis of rotation is automatically specified by the position of the wrist.

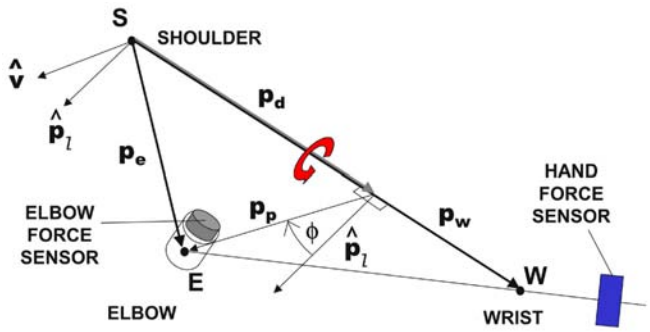

Fig. 4. Self-motion of the arm or "elbow orbit" occurs about a line from the shoulder to the wrist.

TABLE II
ISOLATERAL CONTROL EXERCISES.

Exercise	Plane of Motion	Rotation Axis	Azim./Elev.
Ab/Adduction	frontal	$[1,0,0]$	90°/0°-90°
Flex/Extension	saggital	$[0,1,0]$	0°/0°-90°
Ab/Adduction	transverse	$[0,0,1]$	0°-90°/90°
Elevation	scapula	$[\sqrt{3}/2, 1/2, 0]$	60°/0°-90°
Int/Ext Rotation	⊥humerus	$\overline{SE}$, ${}^B z_U$	−/−
Elbow Orbit	⊥shoulder-wrist	$\overline{SW}$, ${}^0 p_5$	−/−

Some common isolateral exercises are shown in Table II. The second column indicates the plane of motion, and the third column indicates the axis of rotation. The final column specifies the azimuth and elevation of the humerus during the exercise. Azimuth corresponds to the rotation about the longitudinal axis z_B (0° is straight ahead) and elevation is the angle the humerus makes with the longitudinal axis (0° is straight down).

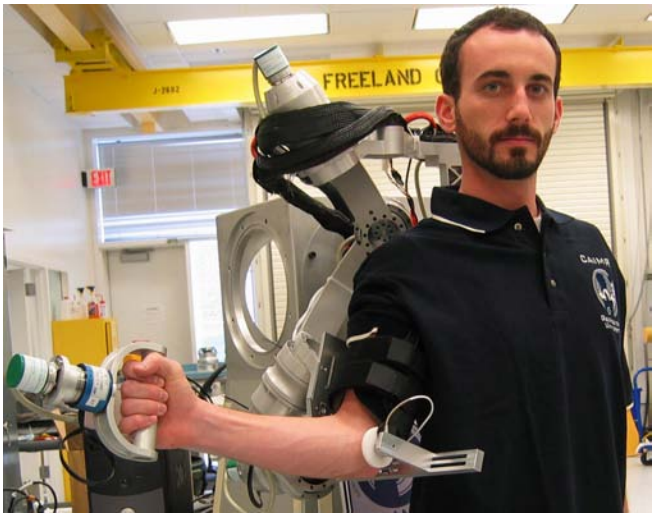

Fig. 5. Exoskeleton shown performing external/internal rotation at about 90° elbow flexion.

Exercises are implemented using the modular "composite" control architecture shown in Figure 7 [4]. The exoskeleton joints are first parsed into mutually exclusive sets of subcontrollers based on the activation of human arm joints during

Fig. 6. Exoskeleton shown at 90° shoulder abduction.

the exercise: scapula (Sc), shoulder (GH), elbow orbit (EO), elbow pitch (EP), and wrist translation (XW). Only certain combinations are allowed; for example, shoulder GH/elbow pitch or wrist translation/elbow orbit are permitted, but not wrist translation/shoulder GH because they have overlapping joints. Each of these joint sets can be selected to operate in either impedance or admittance mode depending upon the desired impedance values. The joint servo modes are set by the composite controller to accept either position or torque commands from the corresponding subcontroller. The shoulder GH controllers are discussed in more detail below.

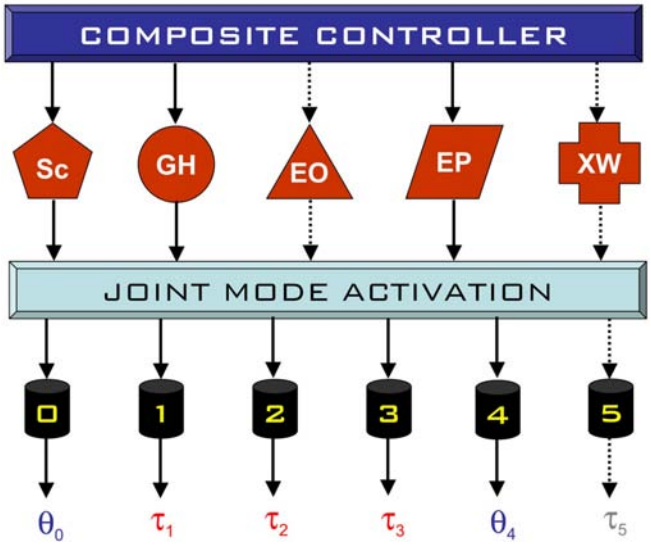

Fig. 7. The Sc Admittance, GH Impedance, and EP Admittance modules are shown here being enabled by the composite controller for a shoulder rotation exercise. The Sc and EP output scapula and elbow position commands, respectively, whereas the GH module outputs shoulder torque commands. A joint mode command of either "position" or "torque" is sent to each motor servo by the composite controller to enable the appropriate input. (Subcontrollers: Sc=scapula, GH=glenohumeral, EP=elbow pitch, EO=elbow orbit, XW=wrist translation.)

A. Shoulder Impedance Module

The shoulder impedance controller is primarily used for low resistance shoulder rotation exercises. The desired impedance is multiplied by the angular velocity of the glenhumeral (GH) joint shown in Figure 8 to produce a desired Cartesian torque T_{des}. The desired torque and "sensed" torque are then "differenced" to form a torque error and multiplied by a feedback gain K_F. The desired torque and feedback error are then converted back to joint coordinates to produce a desired torque τ_{des}. The desired torque and feedforward compensation τ_{fwd} are then summed to form the control command τ to the motors.

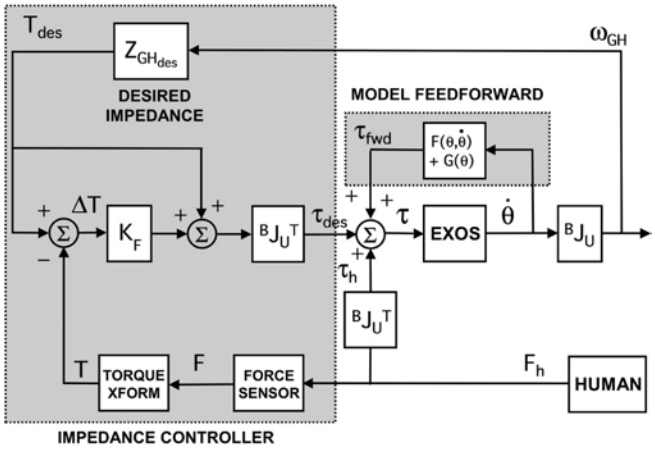

Fig. 8. Impedance controller used for shoulder axis rotation.

The desired stiffness and damping are set in $Z_{GH_{des}}$ to have the specified values about the axis of rotation and high values about the off-axes to maintain isolateral rotation. The z-axis of a rotation frame $\{C\}$ is aligned with the desired axis of rotation, and then ${}^{B}R_{C}$ is the transformation between the rotation frame and the body frame. Thus, the desired stiffness in $Z_{GH_{des}}$ can be found from

$$K_{GH_d} = {}^{B}R_C K_C {}^{B}R_C^T \tag{3}$$

where K_C is the stiffness in the rotation frame (same for damping). If the rotation is about the humeral axis, then the z-axis of the compliance frame aligns with the humerus longitudinal axis so that ${}^{B}R_C = {}^{B}R_U$.

B. Shoulder Admittance Module

The shoulder admittance controller is shown in Figure 9. The elbow and hand force torque sensors are used to derive the humerus and the azimuth-elevation torques. The desired admittance is then multiplied by either the humerus or az-el torques to produced the desired rotational velocity of the shoulder in the base frame, ω_d. The desired Cartesian velocity is then multiplied by the inverse Jacobian to obtain the desired velocities of the shoulder joints $\dot{\theta}_{S_d}$. The desired velocity is then integrated and fed into a joint PD controller to drive the exoskeleton joint angles to the desired positions. Since the torques in the human glenohumeral joint cannot be directly measured, the shoulder torque inputs in Fig. 9 must be estimated using force sensors mounted at the arm-exoskeleton interfaces. The estimation of shoulder torques is discussed in the next section.

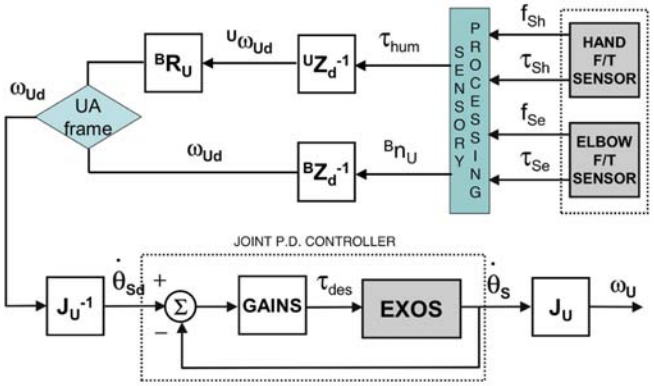

Fig. 9. The admittance controller for the shoulder uses force inputs from the elbow and hand force sensors to compute the commanded shoulder rotational velocity based on the desired admittance.

V. SHOULDER TORQUE ESTIMATION

The force sensors located at the hand and elbow interfaces can be used to estimate the shoulder torques for the admittance controller shown in Fig. 9. For general shoulder rotations, the shoulder torques can be decomposed into those perpendicular to the humeral axis and those about the humeral axis. The perpendicular torques are determined using the elbow sensor, and torques about the humerus axis are more accurately estimated using the hand sensor.

A. Azimuth/Elevation Torques

The shoulder azimuth and elevation torques are estimated by projecting the force and moment from the elbow sensor to frame $\{0\}$. The elbow force and moment in the sensor frame, f_{S_e} and n_{S_e}, are first converted to the upper arm frame using

$$^{U}f_{U} = {}^{U}R_{S_e} f_{S_e} \quad (4)$$

$$^{U}n_{U} = {}^{U}p_{S_e} \times {}^{U}f_{U} + {}^{U}R_{S_e} n_{S_e} \quad (5)$$

where $^{U}p_{S_e} = [0\ 0\ L_{S_e}]^T$ and $^{U}R_{S_e} = R_Z(45°)$ represent the fixed position and orientation of the elbow sensor in frame $\{U\}$. The moment in frame $\{0\}$ is then found from (4) and (5) using

$$^{0}n_{U} = {}^{0}p_{U} \times {}^{0}R_{U}{}^{U}f_{U} + {}^{0}R_{U}{}^{U}n_{U} \quad (6)$$

where $^{0}p_{U} = {}^{0}p_{4}$. The moment can then be converted to frame $\{B\}$ coordinates through pre-multiplying (6) by $^{B}R_{0}$.

B. Humeral Torque

The torque about the upper arm is found from the component of the hand force that is tangent to the humeral axis, i.e. the z_4 direction. The hand sensor is fixed to frame $\{5\}$ at a distance L_{S_h} along the z_5-axis and oriented at an angle $45°$ about z_5 so that $^{5}p_{S_h} = [0\ 0\ L_{S_h}]^T$ and $^{5}R_{S_h} = R_Z(45°)$. The hand sensor force in frame $\{4\}$ is found from

$$^{4}f_{5} = {}^{4}R_{5}{}^{5}R_{S_h} f_{S_h} \quad (7)$$

where f_{S_h} is the sensor reading. The humeral torque is found using the sensor's z-force and the perpendicular component of the forearm relative to the upper arm

$$\tau_{UA} = (L_F + L_{S_h}) sin(\theta_4)^4 f_5 \bullet \hat{z} \quad (8)$$

where θ_4 is the elbow flexion.

C. Elbow Orbit Torque

The z-component of the elbow force sensor in f_{S_e} can also be used to determine the torque, τ_ϕ, exerted about the shoulder-wrist axis, p_w. The elbow orbit torque is calculated by taking the product of the the z-component of the force and multiplying it by the moment arm

$$\tau_\phi \equiv \mid p_p \mid f_{S_e} \bullet \hat{z} \quad (9)$$

where p_p is the minimum distance from the elbow to $\overline{SW}$.

VI. SHOULDER EXPERIMENTS

Several experiments were conducted to validate the operation of the shoulder and elbow orbit admittance modules during simulated exercises. Since a feedforward model for the exoskeleton is still under development, the impedance module was not tested. The scapula joint was maintained at $0°$ throughout these tests.

A. Shoulder Abduction Experiment

The shoulder admittance controller was used to program a constant resistance during a lateral raise exercise in the scapula plane. The upper arm was initially oriented straight down by the side at $0°$ elevation parallel to z_B but with the x_U-axis rotated inward approximately $30°$ about the $+z_B$-axis. The upper arm was then elevated about the x_U-axis to a horizontal position similar to that shown in Figure 6. The desired stiffness was set to $k_{diag} = [0\ 500\ 500]$ N-m/rad so that it was free to rotate about the x_U-axis but stiff in the off-axis directions. The desired damping was set to $b_{diag} = [100\ 500\ 500]$ N-m/rad/sec so that the desired impedance about the x_U-axis was pure viscous damping.

The resulting angular displacement and rate are shown in Figure 10. The angle decreases in magnitude as the humerus elevates to a horizontal position, and then reverses direction as it descends. The shoulder torque estimated using the elbow sensor is shown in Figure 11. The torque is predominantly about the rotational axis x_U and reaches a peak of about 20 rad/sec. The velocity during the abduction phase is approximately 0.2 rad/sec, which would be expected to produce a torque of approximately $b_d\omega$=20 N-m which agrees with the actual values shown in Figure 11.

B. Self-Motion Experiment

In this experiment, the subject executes a pure elbow orbit maneuver by "rolling" the elbow about the shoulder-wrist line first counterclockwise and then clockwise as viewed from the shoulder. The desired elbow orbit impedance was set to be a pure rotational damping of $Z_{\phi_{des}} = 50$ N-m/rad/sec so that the exerted torque should be proportional

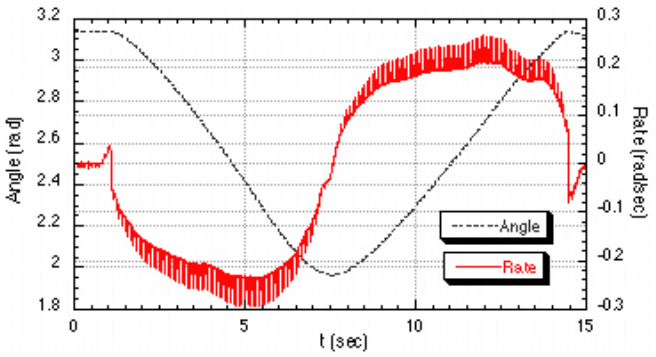

Fig. 10. Eigen-axis angle and rate during lateral abduction.

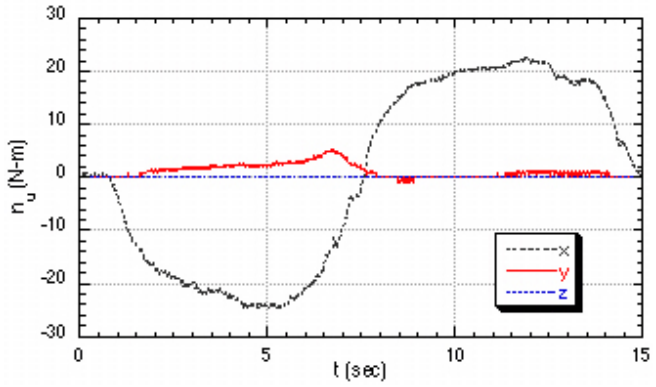

Fig. 11. Torques in the shoulder during lateral abduction.

to the rotational velocity. The resulting elbow orbit angle and torque are shown in Figure 12. The slope of the elbow orbit angle is approximately constant giving an angular velocity of about 0.1 rad/sec. The torque flips signs as the direction of rotation changes yielding a value of about 5 N-m during the maneuver.

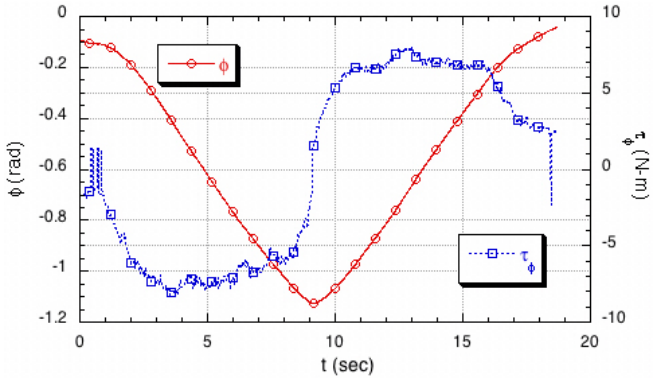

Fig. 12. Elbow orbit angle and torque for $b_\phi = 50$ N-m/rad/s during accommodation maneuver.

VII. CONCLUSION

Rotational kinematics were developed for controlling the shoulder joints of an arm exoskeleton for several isolateral exercise protocols. A torque estimation scheme based on dual force sensors was used to supply torque input to the shoulder GH admittance controller. The admittance controller demonstrated good ability to track a pure damping impedance for isolateral rotation or elbow orbit, which does not rely on model feedforward. Although the shoulder GH impedance controller has also been coded, gravity and friction feedforward models need to be developed before the controller can be used.

Work is currently in-progress to fully develop the other control modules so that a full cadre of exercise protocols can be implemented. Impedance parameters are being determined for a variety of exercise protocols that take into account the human strength potentials over the range of motion. In addition, VR protocols are also being created to implement functional training and proprioceptive neuromuscular facilitation (PNF) patterns. After the protocols have been developed, clinical trials will be conducted and compared with results from manual therapy and passive exercise machines.

ACKNOWLEDGMENT

Thanks go to Mike Liszka, John Tang, Emmanuel Wilson, and Mike Perna for their engineering support on the MGA Exoskeleton. This project was sponsored by the U.S. Army Telemedicine and Advanced Technology Research Center (TATRC) under Grant #W81XWH-04-1-0078.

REFERENCES

[1] G. C. Burdea, *Force And Touch Feedback For Virtual Reality*. New York: John Wiley and Sons, 1996.

[2] C. Carignan and K. Cleary, "Closed-loop force control for haptic simulation of virtual environments," *The Electronic Journal of Haptics Research (http://www.haptics-e.org)*, vol. 2, no. 2, pp. 1–14, Feb. 2000.

[3] C. Carignan and D. Akin, "Achieving impedance objectives in robot teleoperation," in *Proc. of the IEEE Conference on Robotics and Automation*, 1997, pp. 3487–3492.

[4] C. Carignan, J. Tang, S. Roderick, and M. Naylor, "A configuration-space approach to controlling a rehabilitation arm exoskeleton," in *Int. Conf. on Rehabilitation Robotics (ICORR)*, Noordwijk, Netherlands, June 2007, pp. 179–187.

[5] C. Clover, G. Luecke, J. Troy, and W. McNeely, "Dynamic simulation of virtual mechanisms with haptic feedback using industrial robotics equipment," in *Proc. of the IEEE Conference on Robotics and Automation*, Apr. 1997, pp. 724–730.

[6] J. Craig, *Introduction to Robotics: Mechanics and Control, 2nd ed.* Reading, Mass.: Addison-Wesley, 1989.

[7] A. Frisoli, F. Rocchi, S. Marcheschi, A. Dettori, F. Salsedo, and M. Bergamasco, "A new force-feedback arm exoskeleton for haptic interaction in virtual environments," in *Proc. of the First Joint Eurohaptics Conference and Symposium on Haptic Interfaces for Virtual Environment and Teleoperator Systems*, 2005, pp. 195–201.

[8] K. Kreutz-Delgado, M. Long, and H. Seraji, "Kinematic analysis of 7 DOF manipulators," *Int. Journal of Robotics Research*, vol. 11, no. 5, pp. 469–481, 1992.

[9] D. Lawrence, "Impedance control stability properties in common implementations," in *Proc. IEEE Int. Conf. on Robotics and Automation*, 1988, pp. 1185–1190.

[10] T. Massie and J. K. Salisbury, "The PHANTOM haptic interface: A device for probing virtual objects," in *Proc. ASME Winter Annual Meeting: Symposium on Haptic Interfaces for Virtual Environment and Teleoperator Systems*, vol. DSC 55-1, Nov. 1994, pp. 295–300.

[11] A. Nakai, Y. Kunii, H. Hashimoto, and F. Harashima, "Arm type haptic human interface: Sensor arm," in *Intl. Conf. on Artificial Reality and Tele-Existence (ICAT)*, Tokyo, Japan, Dec. 1997, pp. 77–84.

[12] T. Nef, M. Mihelj, G. Colombo, and R. Riener, "ARMin – robot for rehabilitation of the upper extremities," in *Proc. IEEE Int. Conf. on Robotics and Automation*, orlando, 2006, pp. 3152–3157.

[13] L. Peterson and P. Renstrm, *Sports Injuries Their Prevention and Treatment, 3rd ed.* Champaign, Il.: Human Kinetics, 2001.